Blind Image Quality Assessment designed by learning-based attributes selection

Christophe Charrier [1], *Abdelhakim Saadane* [2], *Christine Fernandez-Maloigne* [3]

[1] *Normandie Univ, UNICAEN, ENSICAEN, CNRS, GREYC, 14000 Caen, FRANCE*

[2] *Université de Nantes, XLIM UMR CNRS 7252*

[3] *Université de Poitiers, XLIM UMR CNRS 7252*

Abstract

With the rapid growth of image processing technologies, objective Image Quality Assessment (IQA) is a topic where considerable research effort has been made over the last two decades. IQA algorithms based on image structure have been shown to correlate well with Mean Opinion Scores (MOS). No-Reference (NR) image quality metrics are of fundamental interest as they can be embedded in practical applications This paper deals with a new NR-IQA metric based on natural scenes statistics. It proposes to model the best correlated statistics of seven well known no-reference image quality algorithms by a MultiVariate Gaussian Distribution (MVGD). A part of LIVE database is used with the associated DMOS to fit the MVGD model, namely Model Image Quality Index (MIQI). Hence, the quality of a distorted image is given by the DMOS that maximizes the multivariate Gaussian probability density function. Experimental results demonstrate the method effectiveness for a wide variety of distortions.

Introduction

The rapid development of image and video processing technologies and the exponential increase in the demand of new multimedia services raise the critical issue of assessing the visual quality. To meet this need, reliable methods have been developed. Since the human observer is the ultimate judge, subjective assessment when properly implemented [1, 2] is the most accurate method to evaluate the visual quality but is time consuming and unsuitbale for real-time applications. Objective IQA algorithms [3] aim at predicting image quality from objective features extracted from images. Two approaches are generally considered in the design of objective IQA algorithms : (i) the visually based approach that aims to mimic the human visual system behavior and (ii) the signal based approach that extracts and analyses features in image signals. Signal based approaches which represent the context of this paper, present a good tradeoff between performance and complexity. Generally, these approaches require two steps. In the first one, relevant features are extracted while, in the second, these features are pooled in order to produce the quality score of the image under test. The first step has been the subject of several investigations [4, 5, 6]. In contrast, the second step still uses conventional combinations. To avercome this drawback, statistical modeling of natural images has been considered and has been shown to correlate well with perceived quality as measured by subjective assessment. Statistical modeling is based on the assumption that natural scenes belong to a specific subspace within which all the images evolve. In the case of no-reference metrics, the features extraction procedure is followed by a learning step.
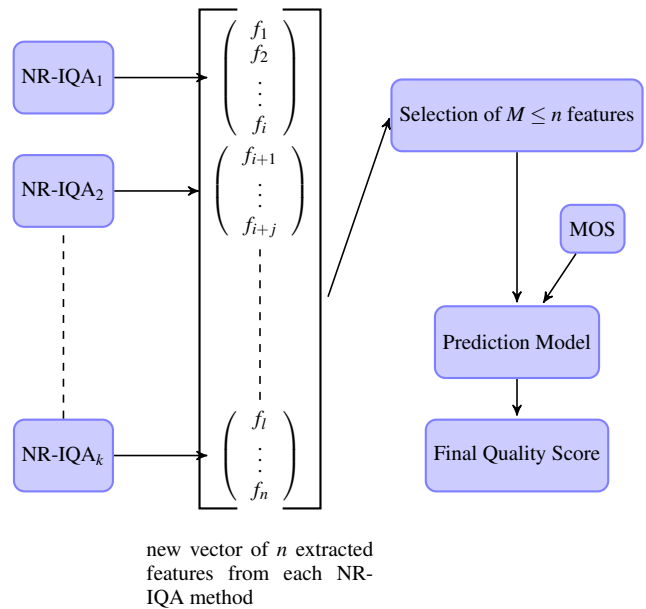

new vector of n extracted features from each NR-IQA method

Figure 1. *General scheme of the proposed NR-IQA algorithm based on combination of features.*

When a large ground truth is available, the learning methods can efficiently map features and MOS [7, 8, 9, 10, 11]. Instead of looking to define new features, this paper will exploit the features of seven well-known metrics. These features are then sorted regarding their specific correlation coefficient. The most correlated ones are then used by the learning step to fit a multivariate gaussian distribution (MVGD). This MVGD handles the features of a given distorted image to assess its quality. This paper is organized as follows. Section 2 describes the extracted features. Section 3 presents the proposed method and section 4 gives the experimental results.

Features description

All features considered in this paper are extracted from nine commonly used learning-based NR-IQA learning-based metrics : 1) BRISQUE [12], 2) BLIINDS [13], 3) BLIINDS-II [14], 4) NIQE [15], 5) DIIVINE [16], 6) BIQI [11], 7) IL-NIQE [17], 8) SSEQ [18] and 9) OG-IQA [19]. A second reason of the choice of those trial algorithms is motivated by the fact that the code of all of them is publicly available.

NR-IQA algorithm	Comments	Features	
BRISQUE	Natural scene statistic-based distortion-generic	36	$f_1, \ldots, f_{36}$
BLIINDS	Machine learning-based approach (Probabilistic model)	4	$f_{37}, \ldots, f_{40}$
BLIINDS-II	Machine learning-based approach (Probabilistic model)	4	$f_{41}, \ldots, f_{44}$
NIQE	Space domain natural scene statistic model	35	$f_{45}, \ldots, f_{79}$
DIIVINE	Classification (SVM) and Regression (SVR)	83	$f_{80}, \ldots, f_{162}$
BIQI	Machine learning-based approach (SVM).	4	$f_{163}, \ldots, f_{166}$
IL-NIQE	Global Multivariable Gaussian model	5	$f_{167}, \ldots, f_{171}$
SSEQ	2-stage framework distortion classification and Regression (SVR)	12	$f_{172}, \ldots, f_{183}$
OG-IQA	AdaBoosting back-propagation neural network	6	$f_{184}, \ldots, f_{189}$

Table 1: NR-IQA metrics considered to investigate the relevance of features.

MIQI feature	Selected from	Initial feature	SROCC
a_1	BLIINDS-II	f_{42}	0.924
a_2	ILNIQE	f_{167}	0.842
a_3	ILNIQE	f_{168}	0.840
a_4	ILNIQE	f_{170}	0.815
a_5	BIQI	f_{163}	0.749
a_6	BIQI	f_{166}	0.714
a_7	BLIINDS-II	f_{43}	0.555
a_8	BLIINDS-II	f_{44}	0.550
a_9	BLIINDS-II	f_{41}	0.547
a_{10}	BIQI	f_{164}	0.543
a_{11}	NIQE	f_{48}	0.516
a_{12}	NIQE	f_{51}	0.509
a_{13}	NIQE	f_{56}	0.505
a_{14}	NIQE	f_{52}	0.505
a_{15}	NIQE	f_{55}	0.505
a_{16}	BIQI	f_{165}	0.503
a_{17}	NIQE	f_{63}	0.499
a_{18}	NIQE	f_{59}	0.485

Table 2: SROCC mean values of each selected feature to be used by MIQI (LIVE database).

percentile	10th	100th
MIQI	0.952	0.942

Table 3: SROCC values computed between subjective DMOS and MIQI scores with highest 10th percentile and 100th percentile

MIQI NR-IQA method
General Scheme

All the trial NR-IQA methods applies the same principle: after computing a set of different features, a combination of this set is performed in different ways. In this paper, the design a NR-IQA algorithm is based on a new selection process of relevant attributes provided by different common NR-IQA methods. Fig 1 displays the general scheme of the proposed method. From all trial NR-IQA schemes, all features are computed. This yields to a set of n features. From this initial set a subset of M attributes is generated (under the constraint that $M \leq n$) in order to keep the most relevant features with respect to some criteria. Then from selected criteria, a MultiVariate Gaussian Distribution (MVGD)

is deployed to predict the final score of images.

Selection of features

All previously described features are computed for all original images (and their associated degraded version) of the LIVE IQA database [20]. This database contains 29 original images, each impaired by many levels of 5 distortion types: JPEG2000, JPEG, white noise, Gaussian blur, and fast-fading channel distortions. The total number of distorted images is 779. Then for each feature, the Spearman Rank-Order Correlation Coefficient (SROCC) between values of features and subjective DMOS is computed. Finally, only the highest 10th percentile is considered to design the NR IQA method. Indeed, it has been previously observed that percentile pooling results in high correlations with subjective perception of quality [21, 14]. In addition, percentile pooling is motivated by the fact that the worst distortions in an image dominate subjective impressions. We choose 10% as a round number to avoid the possibility of training.

Table 2 shows the best eighteen features with their corresponding SROCC for the test LIVE image database. It also specifies the NR-IQA algorithms from which, each selected feature is extracted. These features are used to compute MIQI values. We observe that all the 18 selected features only come from four recent NR-IQA methods: BLIINDS-II, IL-NIQE, BIQI and NIQE. The six first parameters show SROCC values greater than 0.7 (0.924 for the higher), that correspond to good to high correlation levels with subjective scores. The remaining features provides SROCC values around 0.5. Thus, all the selected features range from 0.485 to 0.924 including medium to high correlated features with DMOS. One can observe that all features from BLIINDS-II and BIQI have been selected since they present high correlation level with DMOS.

From BLIINDS2, the extracted features are based on a Natural Scene Statistics (NSS) model of DCT coefficients in order to compute the generalized Gaussian Model shape parameter (which allows to capture primary distortion affecting the image quality),the coefficient of frequency variation, the energy subband ratio measure to capture the difference in the local spectral signatures between original and distorted images, and the Orientation Model-Based Feature to capture directional information that may be significant in subjective assessment of quality. THose kind of features are agnostic parameters that do not need any assumption on degradation.

From BIQI, the selected features refer to NSS parameters

Test LIVE subset	BIQI	DIIVINE	BLIINDS	BLIINDS-II	NIQE	BRISQUE	ILNIQE	SSEQ	OG-IQA	MIQI
JP2K	0.802	0.913	0.912	0.943	0.906	0.938	0.953	0.942	0.937	0.965
JPEG	0.879	0.910	0.839	0.954	0.847	0.923	0.843	0.951	0.964	0.959
White Noise	0.958	0.984	0.974	0.980	0.975	0.986	0.972	0.978	0.986	0.985
Gaussian Blur	0.821	0.921	0.957	0.941	0.945	0.978	0.898	0.948	0.961	0.981
Fast Fading	0.730	0.863	0.750	0.933	0.882	0.929	0.787	0.904	0.898	0912
Cumulative subsets	0.824	0.916	0.799	0.912	0.877	0.941	0.468	0.935	0.950	0.952

Table 4: SROCC values computed between predicted scores and MOS values LIVE Images database. Considering MIQI, median SROCC values are computed between predicted scores and MOS values for the 1000 train-test LIVE Images database.

CSIQ subset	BIQI	DIIVINE	BLIINDS	BLIINDS-II	NIQE	BRISQUE	ILNIQE	SSEQ	OG-IQA	MIQI
JP2K	0.708	0.830	0.575	0.895	0.906	0.866	0.906	0.848	0.857	0.914
JPEG	0.867	0.799	0.264	0.901	0.883	0.903	0.899	0.865.	0.923	0.912
Gaussian Noise	0.324	0.176	0.293	0.379	0.299	0.252	0.850	0.872	0.877	0.842
Add. Gaussian Pink Noise	0.879	0.866	0.555	0.801	0.810	0.925	0.874	0.046	0.024	0.933
Gaussian Blur	0.771	0.871	0.774	0.891	0.892	0.903	0.858	0.873	0.893	0.931
Global Contrast Decrement	0.585	0.396	0.078	0.012	0.232	0.029	0.501	0.200	0.467	0.652
Cumulative subsets	0.619	0.596	0.170	0.577	0.286	0.566	0.815	0.528	0.559	0.832

Table 5: SROCC values computed between predicted scores and MOS values for the CSIQ Images database.

computed in the wavelet domain to coarsely mimics the scale-space-orientation decomposition that is assumed to occur in area V1 of the primary visual cortex of the human visual system. The selected features are degradation oriented to score the quality of four sets of images : JPEG and JEPG2000 compressed images, Gaussian blurred and white noisy images.

Considering IL-NIQE, three of the five available features are used to defined MIQI. IL-NIQE is based on constructing a collection of "quality aware" features. Those features are derived from the distribution of locally mean subtracted and contrast normalized (MSCN) feature and are statistics of normalized luminance, statistics of MSCN products and statistics of Log-Gabor Filter Responses to mimic orientation and frequency selectivity of neurons in the visual cortex. The two first are spatial features and the third one is computed in the frequency domain.

Regarding NIQE, the used features are space domain NSS, and correspond to the parameters of asymmetric generalized Gaussian distribution along three orientations plus the mean of the distribution. The main idea is to mimic the human judgment that seems to be more heavily weighted from sharp image regions. Those features are computed in the space domain.

Finally, one observes that features from frequency, spatio-frequency and space domain are used to designed MIQI. Another remark relies to the fact that even if many features are agnostic, degradation-based attributes are also used. A combination of the two sets of attributes seems to be necessary to design a NR-IQA index.

Prediction model

Let $X_i = \{a_1, a_2, \ldots, a_k\}$ be the vector of selected attributes, where i is the index of the image to be assessed. In addition let DMOS_i be the associated subjective DMOS. To model the distribution of (X_i, DMOS_i), a multivariate generalized Gaussian model (MVGD), namely Model Image Quality Index (MIQI), is

used to compute the final score as

$$
\mathrm{MIQI}(x) = \frac{1}{(2\pi)^{k/2} |\Sigma|^{1/2}} \exp\left(-\frac{1}{2} (x-\beta)^T \Sigma^{-1} (x-\beta) \right) \tag{1}
$$

where $x = (a_1, .., a_k, \mathrm{DMOS})$ corresponds to the k most relevant features to which is added the DMOS of training distorted images. β and Σ denote the mean and covariance matrix of the MVGD model and are estimated using the maximum likelihood method. The probabilistic model is trained on a subset of the LIVE IQA database, for which, one has access to DMOS values. To ensure a robustness of results, multiple training sets were constructed. In each, the image database was subdivided into distinct training and test sets (completely content-separate). For each train set, 80% of the LIVE IQA Database content was chosen, inducing that the remaining 20% is considered for the test set. Specifically, each training set contained images derived from 23 original images, while each test set contained the images derived from the remaining 6 original images. 1000 randomly chosen training and test sets were obtained and the prediction of the quality scores was run over the 1000 iterations.

Experimental results
Experimental setup

To evaluate the performance of the proposed IQA algorithm, two other publicly available databases are used: 1) TID2013 database [22] and 2) CSIQ image database [23]. Even if the LIVE database has been used to fit the MVGD model MIQI, TID2013, CSIQ and the 1000 train-test LIVE Images databases will serve as test set.

To perform this evaluation, the SROCC is computed between DMOS values and the scores predicted by the proposed metric and the seven trial NR-IQA algorithms. In this paper, the number of

TID2013 subset	BIQI	DIIVINE	BLIINDS	BLIINDS-II	NIQE	BRISQUE	ILNIQE	SSEQ	OG-IQA	MIQI
Additive Gaussian Noise	0.785	0.855	0.515	0.722	0.819	0.852	0.876	0.807	0.809	**0.897**
Additive Noise in Color Components	0.541	0.712	0.331	0.649	0.670	0.709	0.815	0.681	0.681	**0.815**
Spatially Correlated Noise	0.465	0.463	0.457	0.767	0.666	0.491	**0.923**	0.635	0.095	0.901
Masked Noise	0.494	0.675	0.470	0.512	0.746	0.575	0.512	0.565	0.691	**0.801**
High Frequency Noise	0.877	0.878	0.677	0.824	0.845	0.753	0.868	0.860	0.834	**0.897**
Impulse Noise	0.748	**0.806**	0.637	0.650	0.743	0.630	0.755	0.749	0.597	0.802
Quantization Noise	0.389	0.165	0.653	0.781	0.850	0.798	**0.873**	0.468	0.710	0.859
Gaussian Blur	0.764	0.834	0.664	0.855	0.795	0.813	0.814	**0.858**	0.814	0.854
Image Denoising	0.409	0.723	0.469	0.711	0.590	0.586	0.750	0.783	0.585	**0.831**
JPEG Compression	0.857	0.629	0.771	0.864	0.840	0.852	0.834	0.825	0.867	**0.879**
JPEG2000 Compression	0.733	0.853	0.740	0.898	0.889	0.893	0.857	0.885	0.882	**0.921**
JPEG Transmission Errors	0.304	0.239	0.094	0.117	0.003	0.315	0.282	**0.354**	0.013	0.2321
JPEG2000 Transmission Errors	0.367	0.060	0.289	0.620	0.510	0.360	0.524	0.561	0.138	**0.665**
Non Eccentricity Pattern Noise	0.007	0.060	0.128	0.096	0.070	**0.145**	0.080	0.011	0.066	0.127
Local Block-wise Distortions	0.081	0.093	0.161	0.209	0.127	**0.224**	0.135	0.016	0.075	0.215
Mean Shift	0.035	0.010	**0.279**	0.128	0.163	0.124	0.184	0.108	0.166	0.201
Contrast Change	0.413	0.460	0.036	0.150	0.018	0.040	0.014	0.204	0.094	**0.532**
Change of Color Saturation	0.142	0.068	0.264	0.017	0.246	0.109	0.162	0.074	0.098	**0.498**
Multiplicative Gaussian Noise	0.642	0.787	0.479	0.716	0.694	0.724	0.693	0.679	0.682	**0.791**
Comfort Noise	0.642	0.116	0.229	0.017	0.155	0.008	**0.359**	0.033	0.188	0.358
Lossy Compression of Noisy Images	0.526	0.633	0.641	0.719	0.801	0.685	0.828	0.610	0.656	**0.823**
Color Quantization with Dither	0.698	0.436	0.434	0.736	0.783	0.764	0.748	0.528	0.294	**0.806**
Chromatic Aberrations	0.544	0.661	0.639	0.539	0.561	0.616	0.679	0.688	0.616	**0.692**
Sparse Sampling and Reconstruction	0.760	0.834	0.738	0.816	0.834	0.784	0.865	0.895	0.832	**0.903**
Cumulative subsets	0.294	0.355	0.289	0.393	0.311	0.367	0.494	0.332	0.292	**0.512**

Table 6: SROCC values computed between predicted scores using NR-IQA schemes from which some attributes are extracted to design LEVIQI and MOS values for TID2013 Images database.

	BIQI	DIIVINE	BLIINDS	BLIINDS-II	NIQE	BRISQUE	ILNQE	SSEQ	OG-IQA
MIQI	111111	11-111	11-111	1--101	11-101	11--01	111111	1--1-1	1--1--

Table 7: Statistical significance matrix of NR-IQA/DMOS on test LIVE database subsets. Each entry in the table is a codeword consisting of 1sixsymbols. The position of the symbol represents the tested subsets as {`jp2k, jpeg, white noise, Gaussian blur, fast fading, all`}. Each symbol gives the result of the hypothesis test on the subset: '1' means that the algorithm for the row is statistically better that the algorithm for the column, '0' means it is worse, and '–' means it is indistinguishable.

selected features to design MIQI is 18 since it corresponds to the highest 10th percentile of features.

In Table 3, we report SROCC values between the LIVE DMOS and MIQI scores for the highest 10% and 100% pooled features, respectively. We observe that the correlations are consistently higher when the lowest 10th percentile pooling strategy is adopted. This may be interpreted as further evidence that human sensitivity to image distortions is not a linear function of the distortion. Actually, human being tends to judge small degraded regions in an image more harshly than good ones, and by the way, tends to penalize the whole image quality [21].

In addition, to ascertain which differences between NR-IQA schemes performance are statistically significant, we applied an hypothesis test using the residuals between the DMOS values and the ratings provided by the IQA algorithms. This test is based on the t-test that determines whether two population means are equal or not. This test yields us to take a statistically-based conclusion of superiority (or not) of an NR-IQA algorithm.

Performance evaluation

Table 4 gives SROCC mean values computed between predicted scores and MOS values for the LIVE Images database. For distortions that are similar to the learned ones (JP2K, JPEG, Gaussian blur), using MIQI leads to a better result than using the other NR-IQA algorithms. In all cases, it performs better. Moreover,

it achieves a significant performance gain when considering the Gaussian noise distortion.

Table 5 gives SROCC mean values computed between predicted scores and MOS values for the CSIQ Images database. For distortions that are similar to the learned ones (JP2K, JPEG, Gaussian blur), using MIQI leads to a better result than using the other NR-IQA algorithms. In all cases, it performs better. Moreover, it achieves a significant performance gain when considering the Gaussian noise distortion. For non learnt distortions such as Global Contrast Decrement, MIQI remains very interesting since it outperforms trial algorithms. This tends to demonstrate the generalization capability of the proposed method to score the quality of images.

Table 6 presents results when SROCC is computed between predicted scores and MOS values for the TID13 Images database subsets. This will yield us to measure the generalization capability of the proposed method to score the quality of an image with a high level of confidence when distortions have not learnt. When considering each distortion, one can see that the performance of MIQI equals or, in several cases exceeds all of the NR-IQA metrics on 15 distortions. We observe that some of them have not been learnt such as "contrast change", "Change of color saturation", "Chromatic aberrations" or "Sparse sampling and reconstruction". Yet, MIQI is less efficient on nine degradations including learnt artifact such as "Gaussian Blur". When considering all

	BIQI	DIIVINE	BLIINDS	BLIINDS-II	NIQE	BRISQUE	ILNQE	SSEQ	OG-IQA
MIQI	1111111	1111111	1111111	--11111	-111111	--1-111	---1111	--11111	1-01111

Table 8: Statistical significance matrix of NR-IQA/DMOS on test CSIQ database subsets. Each entry in the table is a codeword consisting of seven symbols. The position of the symbol represents the tested subsets as mentioned in the first column of Table 5. Each symbol gives the result of the hypothesis test on the subset: '1' means that the algorithm for the row is statistically better that the algorithm for the column, '0' means it is worse, and '−' means it is indistinguishable.

	BIQI	DIIVINE	BLIINDS	BLIINDS-II	NIQE	BRISQUE	ILNQE	SSEQ	OG-IQA
MIQI	1	1	1	1	1	1	−	1	1

Table 9: Statistical significance matrix of NR-IQA/DMOS on the entire TID2013 image database.. Each entry in the table is a symbol. The symbol gives the result of the hypothesis test on the subset: '1' means that the algorithm for the row is statistically better that the algorithm for the column, '0' means it is worse, and '−' means it is indistinguishable.

distortions (cumulative subsets line), the overall performance of MIQI is significantly better than that of the other algorithms. The increase of SROCC is about 4% when compared to that of the best algorithm (ILNIQE in this case).

In addition, Table 7 gives obtained results when a One-sided t-test is used to provide statistical significance of NR-IQA/DMOS on the test LIVE database. Each entry in this table is coded using six symbols. The position of each symbol corresponds to one subset of the LIVE database as {jp2k, jpeg, Gaussian noise, Gaussian blur, fast fading, All}. Each symbol gives the result of the hypothesis test on the subset. If the symbol equals '1', the NR-IQA on the row is statistically better than the NR-IQA on the column ('0' means worse, '-' is used when NR-IQAs are indistinguishables).

On can observe that difference between quality scores predicted with MIQI and any trail algorithms is most of the time significant when the entire database is considered or when any subset is used. Even when non learnt distortions are considered, the SROCC difference between MIQI and any trail algorithm is mostly significant.

Table 8 shows similar results when CSIQ database is considered. Most of the time, the quality scores predicted by MIQI is statistically better than the other trial algorithms. For only one degradation (Gaussian noise), OG-IQA is performs better.

Table 9 presents obtained results when a One-sided t-test is used to provide statistical significance of NR-IQA/DMOS on the TID13 database. Only results for the entire database is given. Except for ILNIQE, the difference between the predicted scores provided by MIQI and any other tested NR-IQA method if significant. Considering ILNIQE, the difference is not significant.

Finally, to compare the computational complexity of the proposed algorithm, we measured the average computation time required to assess an image of size 512×578 (using a computer with Intel Core-I7 processor at 2.2GHz). Table 10 reports the measurement results, which are rough estimates only, as no code optimization has been done on our Matlab implementations. It can be observed that the proposed method is highly competitive with faster methods.

Conclusion

In this paper, a new NR-IQA metric is proposed, namely MIQI. The main idea applied to design this new metric is the following: recent NR-IQA metrics predict quality with level of

Algorihm	BIQI	DIIVINE	BLIINDS	BLIINDS-II
time (s)	6.95	38.39	509.82	131.25

Algorihm	NIQE	BRISQUE	ILNIQE	SSEQ
time (s)	0.83	0.75	20.26	22.24

Algorihm	OG-IQA	MIQI		
time (s)	12.65	9.11		

Table 10: Comparison of computational time (in second/image)

correlations with subjective scores, but present high variability of correlation depending on considered degradation that impacts the global correlation rate. Thus selecting highest correlated features with DMOS, one should design one algorithm that provides high correlation value that usual NR-IQA schemes. Thus, MIQI models the best correlated statistics of nine well known algorithms by a multivariate Gaussian distribution.

References

[1] ITU Telecom. Standardization Sector of ITU, *Methodology for the Subjective Assessment of the Quality of Television Pictures, Recommendation ITU-R BT.500-11*, 2004.

[2] ITU Telecom. Standardization Sector of ITU, *Methodology for the Subjective Assessment of the Quality of Television Pictures, Recommendation ITU-R BT.500-10*, August 2000.

[3] D. M. Chandler, "Seven challenges in image quality assessment: past, present, and future research," *ISRN Signal Processing* **2013**, 2013.

[4] Z. Wang, A. C. Bovik, H. R. Sheikh, and E. P. Simoncelli, "Image quality assessment: From error measurement to structural similarity," *IEEE Transactions On Image Processing* **13**(1), pp. 996–1006, 2004.

[5] A. Shnayderman, A. Gusev, and A. Eskicioglu, "An svd-based grayscale image quality measure for local and global assessment," *IEEE Transactions On Image Processing* **15**, pp. 422–429, February 2006.

[6] C. Wee, R. Paramesran, R. Mukundan, and X. Jiang, "Image quality assessment by discrete orthogonal moments," *Pattern Recognition* **43**, pp. 4055–4068, December 2010.

[7] H. Luo, "A training-based no-reference image quality assessment algorithm," in *International Conference on Image Processing (ICIP)*, pp. 2973—2976, 2004.

[8] Y. R. Tsoy, V. G. Spitsyn, and A. V. Chernyavsky, "No-reference image quality assessment through interactive neuroevolution," in *International Conference on Computer Graphics and Vision*, pp. 23–27, 2007.

[9] R. V. Babu, S. Suresh, and A. Perkis, "No-reference JPEG image quality assessment using GAP-RBF," *Signal Processing* **87 (6)**(6), pp. 1493—1503, 2007.

[10] A. K. Moorthy and A. C. Bovik, "Visual importance pooling for image quality assessment," *IEEE J. Selected Topics in Signal Process., Special Issue on Visual Media Quality Assessment* **3**(2), pp. 193—201, 2009.

[11] A. K. Moorthy and A. C. Bovik, "A two-step framework for constructing blind image quality indice," *IEEE Signal processing letters,* **17**(5), pp. 513—516, 2010.

[12] A. Mittal, A. K. Moorthy, and A. C. Bovik, "No-reference image quality assessment in the spatial domain," *IEEE Transactions on Image Processing* **21**(12), pp. 4695–4708, 2012.

[13] M. Saad, A. C. Bovik, and C. Charrier, "A DCT statistics-based blind image quality index," *IEEE Signal Processing Letters* **17**(2), pp. 583–586, 2010.

[14] M. Saad, A. C. Bovik, and C. Charrier, "Blind image quality assessment: A natural scene statistics approach in the dct domain," *IEEE Transactions on Image Processing* **21**(8), pp. 3339–3352, 2012.

[15] A. Mittal, R. Soundararajan, and A. C. Bovik, "Making a "completely blind" image quality analyzer," *IEEE Signal Process. Lett.* **20**(3), pp. 209–212, 2013.

[16] A. K. Moorthy and A. C. Bovik, "Blind image quality assessment: From natural scene statistics to perceptual quality," *IEEE Transactions Image Processing* **20**(12), pp. 3350–3364, 2011.

[17] L. Zhang, L. Zhang, and A. C. Bovik, "A feature-enriched completely blind image quality evaluator," *IEEE Transactions on Image Processing* **24**(8), pp. 2579–2591, 2015.

[18] L. Liu, B. Liu, H. Huang, and A. Bovik, "No-reference image quality assessment based on spatial and spectral entropies," *Signal Processing: Image Communication* **29**, pp. 856–863, 2014.

[19] L. Liu, Y. Hua, Q. Zhao, H. Huang, and A. C. Bovik, "Blind image quality assessment by relative gradient statistics and ada boosting neural network," *Signal Processing: Image Communication* **40**, pp. 1–15, 2016.

[20] Laboratory for Image & Video Engineering, University of Texas (Austin), "LIVE Image Quality Assessment Database," *http://live.ece.utexas.edu/research/Quality* , 2002.

[21] M. H. Pinson and S. Wolf, "A new standardized method for objectively measuring video quality," *IEEE Trans. Broadcasting* **10**, pp. 312–322, Sept 2004.

[22] N. Ponomarenko, L. Jin, O. Ieremeiev, V. Lukin, K. Egiazarian, J. Astola, B. Vozel, K. Chehdi, M. Carli, F. Battisti, and C.-C. J. Kuo, "Image database tid2013: Peculiarities, results and perspectives," *Signal Processing: Image Communication* **30**, pp. 57–77, 2015.

[23] E. C. Larson and D. M. Chandler, "Most apparent distortion: full-reference image quality assessment and the role of strategy," *Journal of Electronic Imaging* **19**(1), pp. 011006–1 – 011006–21, 2010.

Author Biography

Christophe Charrier (M'10) received the M.S. degree from the Nantes University of Science and Technology, Nantes, France, in 1993, and the Ph.D. degree from the University Jean Monnet, Saint-Etienne, France, in 1998. He has been an Associate Professor with the GREYC laboratory at the University of Caen, France, since 2001. In 2008, he was a Visiting Scholar with the Laboratory for Image and Video Engineering, University of Texas, Austin. From 2009 to 2011, he was an Invited Professor with the Computer Department, University of Sherbrooke, Sherbrooke, QC, Canada. He is now the head of the E-Payment & Biometrics research team. His current research interests include digital image and video coding, processing, quality assessment, computational vision, and biometrics data quality.

Abdelhakim Saadane received his Ph.D. degree in Signal Processing and Telecommunications from University of Rennes1. He is currently associate professor at the Polytechnic school of Nantes University and a member of the SIC laboratory in XLIM Institute. His research activities are focused on the Human Visual System modeling and its use in applications such as coding, quality assessment, watermarking and user experience. He is a member of French National Color Imaging Group and serves as a member of division 8 of CIE.

Christine Fernandez-Maloigne is currently Vice-Rector of Poitiers University, in charge of International Relations. She is also director of a CNRS research federation (MIRES), which gathers 560 researchers in the South-West of France, in the area of mathematics, image processing, computer graphic, computer science and communication systems. Her research activities are focused on colour imaging, including fundamental researches about introduction of human visual system models in multiscale colour image processes as well as practical applications. She was co-founder member of the French National Colour Imaging Group (GFINC) in 2000, now part of the CFC (Centre Français de la Couleur). Currenlty, Christine Fernandez-Maloigne is French representative of the CIE Division 8 (Commission Internationale de l'Eclairage, Image Technology Division) since 2006 and secretary of this division since may 2015. She is also deputy Editor-in-chief of JOSA A.